ENVIRONMENTAL RESEARCH
LETTERS

LETTER • OPEN ACCESS

Global mean thermosteric sea level projections by 2100 in CMIP6 climate models

IOP Publishing Environ. Res. Lett. 16 (2021) 014028 https://doi.org/10.1088/1748-9326/abceea

ENVIRONMENTAL RESEARCH
LETTERS

LETTER

Global mean thermosteric sea level projections by 2100 in CMIP6 climate models

Svetlana Jevrejeva[1,2], **Hindumathi Palanisamy**[1] and **Luke P Jackson**[3,4]

[1] Centre for Climate Research Singapore, 36 Kim Chuan Rd., Singapore, Singapore
[2] National Oceanography Centre, Liverpool L3 5DA, United Kingdom
[3] Climate Econometrics, Nuffield College, Oxford University, Oxford OX1 1NF, United Kingdom
[4] Department of Geography, University of Durham, DH1 3LE, United Kingdom

E-mail: svetlana.jevrejeva@gmail.com

Keywords: sea level rise, ocean heat uptake, modelling, future sea level projections

Supplementary material for this article is available online

OPEN ACCESS

RECEIVED
7 August 2020

REVISED
9 November 2020

ACCEPTED FOR PUBLICATION
30 November 2020

PUBLISHED
28 December 2020

Abstract

Most of the excess energy stored in the climate system is taken up by the oceans leading to thermal expansion and sea level rise. Future sea level projections allow decision-makers to assess coastal risk, develop climate resilient communities and plan vital infrastructure in low-elevation coastal zones. Confidence in these projections depends on the ability of climate models to simulate the various components of future sea level rise. In this study we estimate the contribution from thermal expansion to sea level rise using the simulations of global mean thermosteric sea level (GMTSL) from 15 available models in the Coupled Model Intercomparison Project Phase 6 (CMIP6). We calculate a GMTSL rise of 18.8 cm [12.8–23.6 cm, 90% range] and 26.8 cm [18.6–34.6 cm, 90% range] for the period 2081–2100, relative to 1995–2014 for SSP245 and SSP585 scenarios respectively. In a comparison with a 20 model ensemble from Coupled Model Intercomparison Project Phase 5 (CMIP5), the CMIP6 ensemble mean of future GMTSL (2014–2100) is higher for both scenarios and shows a larger variance. By contrast, for the period 1901–1990, GMTSL from CMIP6 has half the variance of that from CMIP5. Over the period 1940–2005, the rate of CMIP6 ensemble mean of GMTSL rise is 0.2 ± 0.1 mm yr^{-1}, which is less than half of the observed rate (0.5 ± 0.02 mm yr^{-1}). At a multi-decadal timescale, there is an offset of $\sim$10 cm per century between observed/modelled thermosteric sea level over the historical period and modelled thermosteric sea level over this century for the same rate of change of global temperature. We further discuss the difference in GMTSL sensitivity to the changes in global surface temperature over the historical and future periods.

1. Introduction

About 93% of the excess energy stored in the climate system due to anthropogenic greenhouse gas emissions has been absorbed by the oceans, leading to thermal expansion and sea level rise (Cheng *et al* 2017, Oppenheimer *et al* 2019). For more than 600 million people living in low-elevation coastal areas future sea level rise is one of the main damaging aspects of climate change (Oppenheimer *et al* 2019). Crucial decisions about adaptation to sea level rise for populous coastal megacities and communities in low lying small islands, where a considerable fraction of global economic activity and critical infrastructure exists, will be made based on future sea level projections (Vousdoukas *et al* 2018, Jevrejeva *et al* 2019, Oppenheimer *et al* 2019, Abadie *et al* 2020).

In a warming climate, global sea level is expected to rise and future sea level projections are made using the conventional method by simulating contributions from individual sea level components, such as thermal expansion, melting ice from glaciers and ice sheets, changes in land water storage and summing them up (Church *et al* 2013, Oppenheimer *et al* 2019). The robustness of and confidence in projections of future sea level change depends on the ability of climate models to reproduce the components of

sea level rise over the 20th century and simulate future changes across a range of emission scenarios (Church *et al* 2013, Oppenheimer *et al* 2019). New results for all sea level components under the most recent climate scenarios will be simulated by, or derived from results in the new Coupled Model Intercomparison Project Phase 6 (CMIP6) (Eyring *et al* 2016), including future contribution from the ice sheets in Ice Sheet Model Intercomparison Project for CMIP6 (Nowicki *et al* 2016).

In this study we analyse global mean thermosteric sea level (GMTSL), one of the components of sea level rise, resulting from thermal expansion due to heat uptake of the ocean. Developing a better understanding of heat uptake and heat transport by the ocean are crucial to simulate the climate system response to the radiative forcing in climate models (Church *et al* 2013, Oppenheimer *et al* 2019, Zanna *et al* 2019, Gregory *et al* 2020). Furthermore, increasing our understanding of large uncertainty in the components of future sea level rise, including the GMTSL, is crucial for effective communication of sea level projections to policy makers, coastal engineers and the general public (Jevrejeva *et al* 2019, Oppenheimer *et al* 2019).

Our main objective is to estimate the thermosteric contribution of future global sea level rise from a new generation of climate models and new scenarios, SSP245 and SSP585 (Eyring *et al* 2016, O'Neill *et al* 2016). We evaluate the CMIP6 simulations of GMTSL against available observations (Ishii and Kimoto 2009, Levitus *et al* 2012, Cheng *et al* 2019) to assess the performance of the CMIP6 models. In addition, we compare GMTSL projections to the Coupled Model Intercomparison Project Phase 5 (CMIP5) outputs previously used for sea level projections (Taylor *et al* 2012, Yin 2012, Church *et al* 2013, Kopp *et al* 2014, Jackson and Jevrejeva 2016, Slangen *et al* 2017). Climate models considered in this study are atmosphere–ocean coupled general circulation models (AOGCMs) and Earth system models (ESMs) from the CMIP6 archive (Eyring *et al* 2016).

We expect CMIP6 GMTSL projections to be different to those of CMIP5 due to a new generation of climate models (e.g. Eyring *et al* 2016), as well as a new set of scenarios of concentrations, emissions, and land use (O'Neill *et al* 2016). We discuss the differences between GMTSL projections, suggesting several explanations for large uncertainties in simulation of GMTSL. Our study demonstrates the need to further improve climate model performance given the importance of oceans in the storage and redistribution of heat defining future climate change (Church *et al* 2013, Winton *et al* 2013, Melet and Meyssignac 2015, Cheng *et al* 2019, Oppenheimer *et al* 2019, Zanna *et al* 2019).

2. Data and method

2.1. Global mean thermosteric simulations in CMIP6

We analyse GMTSL simulations from 15 climate models that are directly available as 'zostoga' in the CMIP6 database (https://esgf-node.llnl.gov/search/cmip6/; Eyring *et al* 2016). Zostoga in CMIP6 models represents a part of the global mean sea level change due to changes in ocean density arising from changes in temperature (Griffies *et al* 2016, Gregory *et al* 2019). Table SI1 (available online at stacks.iop.org/ERL/16/014028/mmedia) displays the list of all 15 CMIP6 models currently available and used in this study. We use 'historical' simulations for the period 1850–2014 (Eyring *et al* 2016) and scenarios SSP245 and SSP585 simulations for the period 2015–2100. The new scenarios are based on a matrix that uses the shared socioeconomic pathways (SSPs) and forcing levels of the Representative Concentration Pathways (RCPs) discussed in O'Neill *et al* (2016). SSP245 and SSP585 correspond to RCP4.5 and RCP8.5 in the CMIP5 framework respectively. Only the first ensemble member 'r1i1p1f1' of the 15 CMIP6 models have been used for both historical and future scenarios. In cases where models provide 'f2' instead of 'f1', that particular forcing was used. We apply a drift correction calculated from the full length pre-industrial control run corresponding to each climate model, for GMTSL simulations following the approach by Sen Gupta *et al* (2013) (see SI).

2.2. GMTSL simulations in CMIP5

The zostoga 'historical' simulations and simulations with RCP4.5 and RCP8.5 future scenarios from 20 CMIP5 models are used in this study (see table SI2 for model information). The 'historical' simulation spans 1850/1860–2005, while the RCPs span 2006–2100. As in the case of CMIP6, only the first member ensemble 'r1i1p1' was used for both historical and RCP simulations. Models were drift corrected following the same method as that for CMIP6 (see SI).

2.3. GMTSL from observations

We compare historical CMIP6 and CMIP5 simulations with updated observational GMTSL datasets from Levitus *et al* (2012), Ishii and Kimoto (2009) and Cheng *et al* (2019) that cover the upper 2000 m of ocean depth. Prior to the 1960s, limited observational data exists from which to estimate GMTSL. Observations of ocean temperature have become more available since this time, providing near global coverage of the ocean. In this study, we estimate the ensemble mean of the Ishii and Kimoto, Cheng, and Levitus GMTSL time series from 1957 to 2005. An updated single time series of steric sea level since 1940 (Cheng *et al* 2019) was used to better constrain the assessment

of GMTSL from the CMIP climate models. The websites for data access are provided in SI.

Three principal time periods have been used to compare and analyse CMIP6 model spread with CMIP5 and observational data: (a) historical simulations from 1901 to 1990 (Oppenheimer *et al* 2019); (b) 1957–2005 corresponding to the beginning of observational records and end of CMIP5 historical simulations; (c) 2015–2100 corresponding to future projections (Oppenheimer *et al* 2019). Estimates 'by 2100' are calculated for the period 2081–2100 relative to 1995–2014.

3. Results

3.1. GMTSL simulations

Using 15 CMIP6 model simulations we compute a multi-model ensemble mean (MEM) for GMTSL rise of 18.8 cm with the 5–95th percentile of 12.8–23.6 cm for SSP245, and a MEM of 26.8 cm with the 5–95th percentile of 18.6–34.6 cm for SSP585 for the period 2081–2100 relative to 1995–2014 (figure 1(a), table SI1). Figure 1(b) displays the MEM simulated by 20 CMIP5 models (table SI2). The models in both frameworks are presented relative 1995–2014. For the historical period CMIP6 and CMIP5 model simulations are plotted as coloured lines with MEM shown as black thick line. The red and blue lines since 2015 and 2005 (figures 1(a) and (b)) indicate the MEM of the CMIP6 and CMIP5 future projections with SSP245/RCP4.5 and SSP585/RCP8.5 scenarios. The shaded regions represent the spread between the 5th and 95th percentile in the CMIP MEMs.

We analyse the difference between the CMIP6 and CMIP5 MEMs of GMTSL in 'historical' simulations and for the future projections with SSP245/RCP4.5 and SSP585/RCP8.5 scenarios respectively (figure SI1). While there is a broad agreement between the CMIP6 and CMIP5 MEMs over the projection period, a clear discrepancy occurs between the two MEMs during the historical period. The considerable disagreement between the model simulations is also reflected in the magnitude of 5–95th percentile ranges in the CMIP6 and CMIP5 models. By 2100 CMIP6 model simulations show larger spread compared to the CMIP5, though the two overlap considerably (figure 1). Over the 1901–1990, the CMIP6 the 5–95th percentile range is nearly half that of CMIP5 (figure SI1).

Although a portion of their uncertainties overlap the CMIP5 ensemble contains a greater number of models (20) than CMIP6 (15). We test the hypothesis that the trend estimated for the MEM from CMIP5 is statistically distinct from that of CMIP6 by randomly drawing a subset from the 20 models in CMIP5 and estimating each MEM. We perform a bootstrap analysis by randomly sampling all combinations of 15 out of 20 CMIP5 models. This is then used to estimate the ensemble mean and compare with the ensemble mean of CMIP6 models. All possible combinations (>15 000) of 15 CMIP5 models were used. Figure 2 shows trend histograms of the MEM GMTSL from these 15 randomly selected CMIP5 models over three time periods: 1901–1990, 1957–2005 and 2015–2100 (RCP8.5/SSP585 projections used here). The ensemble mean CMIP6 (red) and observational GMTSL (black) trends are also displayed as vertical lines. Figures 2(a) and (b) shows that over the historical time period the rate of the CMIP6 MEM is distinctly smaller than the CMIP5 MEM, irrespective of which 15 models are selected from CMIP5. We point out here that the range of CMIP5 MEMs of GMTSL most of the time overestimates the observational trend (figure 2(b); figure SI2, in which the uncertainty for the trend in observations are included). This result contrasts with the projection period (figure 2(c)) where the rate of MEM GMTSL from CMIP6 is larger than all combinations of CMIP5 MEMs.

Table 1. GMTSL rates for the period 1901–1990 and 2015–2100 future scenarios SSP245/RCP4.5 and SSP585/RCP8.5. The rate uncertainty (2 sigma) is calculated using a Monte Carlo method described in section 3.1.

Experiment	Time period	CMIP6 rate (mm yr^{-1})	CMIP5 rate (mm yr^{-1})
Historical	1901–1990	0.2 ± 0.1	0.3 ± 0.1
SSP245/RCP4.5	2015–2100	2.4 ± 0.3	2.1 ± 0.8
SSP585/RCP8.5	2015–2100	3.6 ± 1.2	3.3 ± 1.1

The CMIP6 MEM shows a higher rate of GMTSL rise than the CMIP5 MEM over the future projections for both the scenarios (table 1). In the case of the historical simulations (period 1901–1990), the CMIP6 MEM rate is lower than that of the CMIP5 ensemble. The uncertainties of the rate of the CMIP6 and CMIP5 MEM, as shown in the table 1, are evaluated using Monte Carlo methodology. Around 10 000 random time series are produced by sampling a normal distribution centred on the ensemble mean time series. The uncertainty of the trend is then defined as two times the standard deviation of the normal distribution of the trends of the sampled time series (corresponding to the 95% confidence interval).

While these results reveal that both MEMs are distinct (figure 2), their variances overlap considerably (figure SI1). Visually (figure SI1) it appears that the variance of CMIP6 is smaller than of CMIP5 in the historical period, but larger than CMIP5 for both future scenarios. We evaluate the statistical significance of the CMIP6 variance relative to the variance in CMIP5 by again considering the difference in the number of the available models for CMIP6 and CMIP5 (figure SI3). For future GMTSL projections the CMIP6 variance is larger compared to the variance in CMIP5 and there is no intersection with the range of possible variances estimated from CMIP5 model subsets. We calculate the relative uncertainty

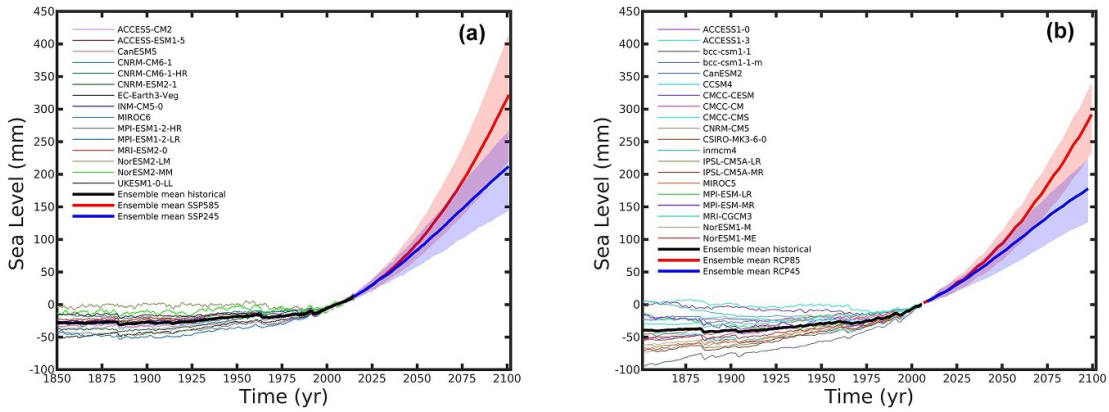

Figure 1. GMTSL (zostoga) for (a) CMIP6 and (b) CMIP5 models from 1850 to 2100 (relative to 1995–2014) using two future scenarios SSP245/RCP4.5 (blue) and SSP585/RCP8.5 (red). Model ensemble mean for 'historical' period is thick black line. Model ensemble mean for SSP585/RCP8.5 and SSP245/RCP4.5 are thick red and blue lines respectively. Shaded areas represent 5–95th percentiles of model ensembles.

(the variance divided by the median versus time) of CMIP6 and CMIP5 GMTSL for historical and projected periods (figure 3). For future projections, the relative uncertainties in both CMIP6 and CMIP5 models are almost constant over time, and independent of scenario for each CMIP respectively. Unlike the projection period, CMIP6 and CMIP5 show relative uncertainties that are time varying and non-linear over the historical period.

3.2. Comparison with observational GMTSL

We compare GMTSL ensemble mean from CMIP6 models with the ensemble mean of three observational datasets (Ishii, 0–2000 m; Levitus, 0–2000 m and Cheng, 0–2000 m) over the common time period 1957–2005 (figure 4). The time series are referenced to 1986–2005 to accommodate the CMIP5 GMTSL simulations and its ensemble mean. Figure 4 (table 2) shows that since 1957 (1957–2005) the trend in MEM CMIP6 GMTSL is 0.3 ± 0.1 mm yr^{-1} compared to the trends of observations of 0.5 ± 0.03 mm yr^{-1}; and 0.6 ± 0.2 mm yr^{-1} from MEM CMIP5 GMTSL. The observational data sets do not include a deep ocean contribution of 0.1 ± 0.1 mm yr^{-1} (1990–2000, Purkey and Johnson 2010) though its inclusion would increase the difference between the CMIP6 MEM and observations.

We compare the rate of GMTSL rise from CMIP6 MEM of 0.2 ± 0.1 mm yr^{-1} with observational steric sea level rise rate of 0.5 ± 0.02 mm yr^{-1} (Cheng *et al* 2017) over the period 1940–2005 (table 2), further indicating that CMIP6 models are underestimating observed changes in global steric sea level. There is a caveat in using dataset from Cheng *et al* (2017), as it is global steric sea level estimated from temperature and salinity related density changes; however, in CMIP6 only GMTSL is available and used in our study. Nonetheless, for the global scale the differences between global mean steric and GMTSL are almost negligible (Gregory and Lowe 2000, WCRP Global Sea Level Budget Group 2018, Gregory *et al* 2019). In addition, there is a very limited number of temperature and salinity observations over 1940–1955 and these estimates should be used with caution due to large uncertainty, as has been mentioned in Cheng *et al* (2017). We have also compared our results with the recently published reconstructed thermosteric sea level data from Frederikse *et al* (2020) over 1957–2005 and 1940–2005 (figure SI4). For both of these time periods, CMIP6 MEM shows an underestimation of global thermosteric sea level rate (as in table 2) compared to that from Frederikse *et al* (2020). Over a longer time span between 1900

Table 2. GMTSL trend over two observational periods, 1957–2005 and 1940–2005. Values in bold correspond to ensemble mean.

	Trend (mm yr^{-1})	
	1957–2005	1940–2005
CMIP5 ensemble mean	**0.6 ± 0.2**	**0.4 ± 0.2**
CMIP6 ensemble mean	**0.3 ± 0.1**	**0.2 ± 0.1**
IK, 0–2000 m	0.6 ± 0.02	N.A
Levitus, 0–2000 m	0.5 ± 0.02	N.A
Cheng, 0–2000 m	0.5 ± 0.03	0.5 ± 0.02
Observational ensemble mean	**0.5 ± 0.03**[a]	**N.A**

Note: The observational data sets do not include deep ocean contribution of 0.1 ± 0.1 mm yr^{-1}, available over the period 1990–2000 only, estimated by Purkey and Johnson (2010), which would enlarge the disagreement between the CMIP6 MEM and observations.

[a] The trend uncertainty of ± 0.03 mm yr^{-1} is the statistical uncertainty calculated using Monte Carlo methodology as explained in section 3.1. This uncertainty is likely optimistic as it does not take into account uncertainties associated with lack/sparsity of observations in the earlier part of the record, uncertainties arising due to differences in mapping method, instrument bias corrections and definition of baseline climatology amongst various processing groups.

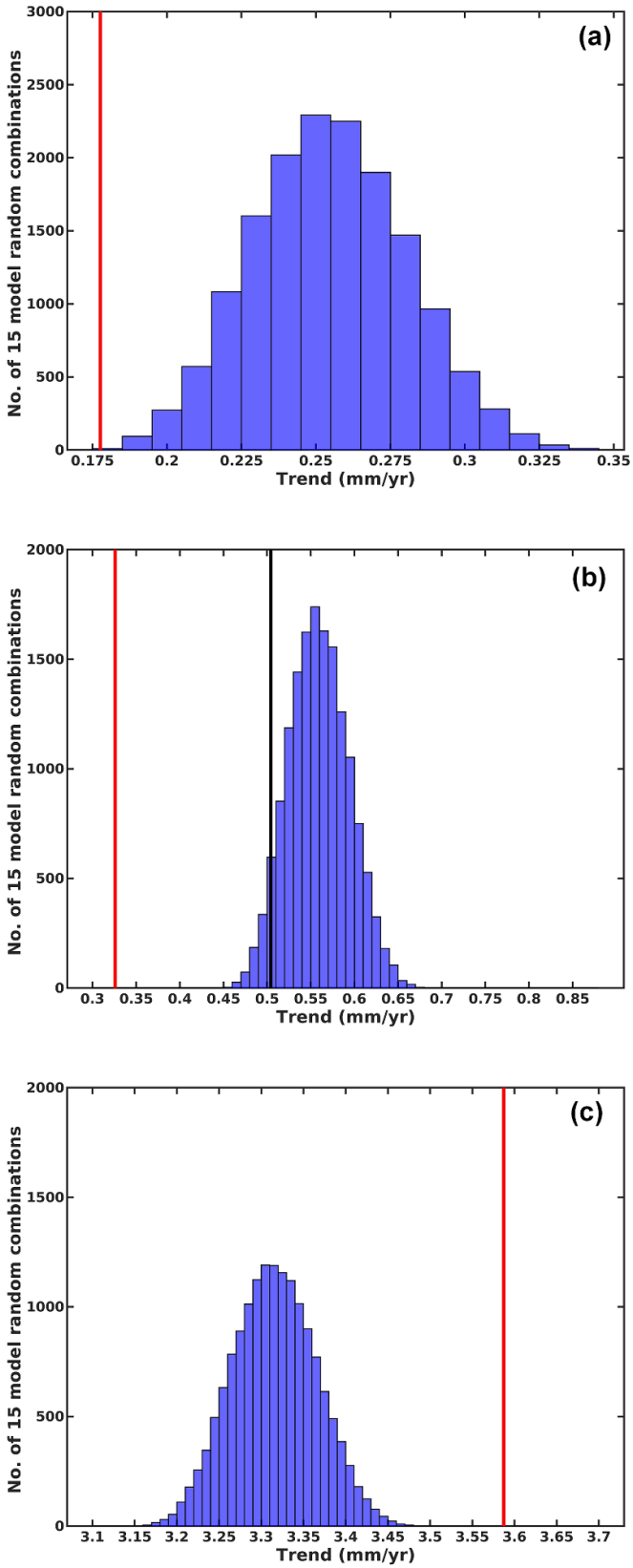

Figure 2. Histogram of CMIP5 MEM GMTSL trends (blue) from all combinations of 15 from 20 models compared to CMIP6 MEM GMTSL trend (red vertical line) over (a) historical period 1901–1990, (b) observational period 1957–2005 and (c) future RCP8.5/SSP585 projections over 2015–2100. Black vertical line (panel b) indicates GMTSL trend from observations (0–2000 m), compare to the model simulations for the full ocean depth.

and 2005 (figure SI4), the reconstructed GMTSL rate from Frederikse *et al* (2020) is 0.45 ± 0.2 mm yr^{-1} and that of CMIP6 MEM is 0.21 ± 0.1 mm yr^{-1}, which is twice smaller than in Frederikse *et al* (2020). Reanalysis estimates from Storto *et al* (2019) show a rate of 0.38 ± 0.04 mm yr^{-1} over 1901–1990.

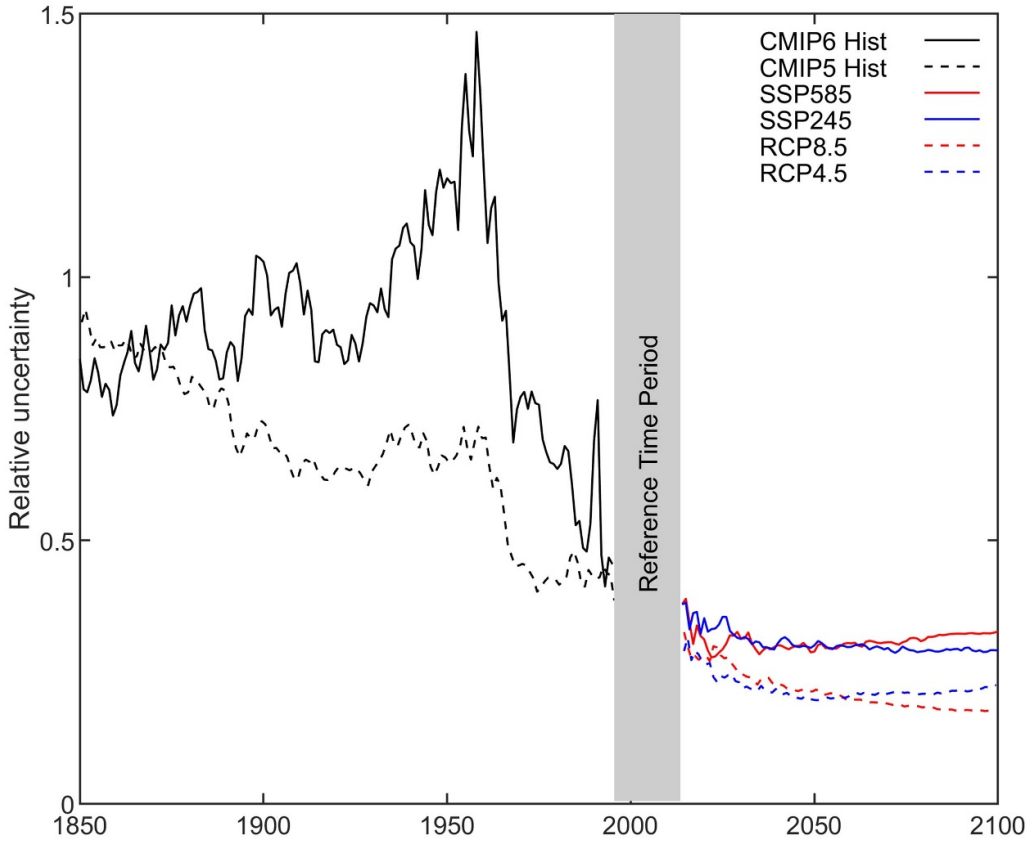

Figure 3. Relative uncertainty, calculated as the ensemble variance divided by the median through time, of CMIP6 and CMIP5 GMTSL for historical and projected periods.

Rate from CMIP6 MEM over the same period is 0.2 ± 0.1 mm yr^{-1}, which is also twice smaller compared to Storto *et al* (2019). These comparisons with reconstructed and reanalysis global mean thermosteric data over longer time show that the CMIP6 MEM is underestimating the observed GMTSL rate.

3.3. GMTSL change as a function of global surface temperature

The delayed response time of the ocean to the forcing means that thermosteric sea level rise in 2100 does not immediately reflect the forcing occurring at that time. Instead the entire pathway since the forcing change was introduced is important (e.g. Bouttes *et al* 2013). Here we consider the relationship between the average rate of GMTSL rise and global surface temperature increase representing the entire preceding century.

We estimate the rate of each model's GMTSL and global surface temperature for CMIP6 and CMIP5 models and their MEMs over the period 1901–1990 and 2015–2100 (figure 5) and introduce a GMTSL sensitivity as a function of the changes in the GMTSL (as rate in cm per century) to changes in global surface temperature (°C per century). To place these results in a wider context we calculate sensitivities of GMTSL as a function of global surface temperature for the 20th century, early deglacial period, and a long-term climate stabilisation case. For the 20th century, we use global temperature reconstructions HadCRUT4 (Morice *et al* 2012) and GISTEMP (Lenssen *et al* 2019, GISTEMP Team 2020) and GMTSL observational datasets (Ishii and Kimoto 2009, Cheng *et al* 2017). For paleo conditions in the early part of the last deglaciation we have used a global temperature reconstruction (Marcott *et al* 2011) and global steric sea level, derived from North Atlantic hosing experiments under this climatology (Fluckiger *et al* 2006). We also estimate GMTSL sensitivity using 1000 year idealised climate model simulations that followed the SRES A1B scenario (close to RCP6.0 scenario) stabilising from 2100 to 3000 (Meehl *et al* 2007). In the latter two cases, while centennial rates of global surface temperature change are comparable to today, the alternate physical mechanism (Fluckiger *et al* 2006) and long-term ocean inertia illustrate contrasting GMTSL responses yet both differ from present-day rates or CMIP projections.

In figure 5 GMTSL sensitivities calculated for CMIP6 (crosses) are generally higher than those for CMIP5 (circles) for all future scenarios. As expected, there is a quasi-linear increase in GMTSL sensitivity to the changes in global surface temperature, which themselves are reflection of changes in both temperature and thermosteric sea level to radiative forcing (e.g. Bouttes *et al* 2013). However, we observe an offset of

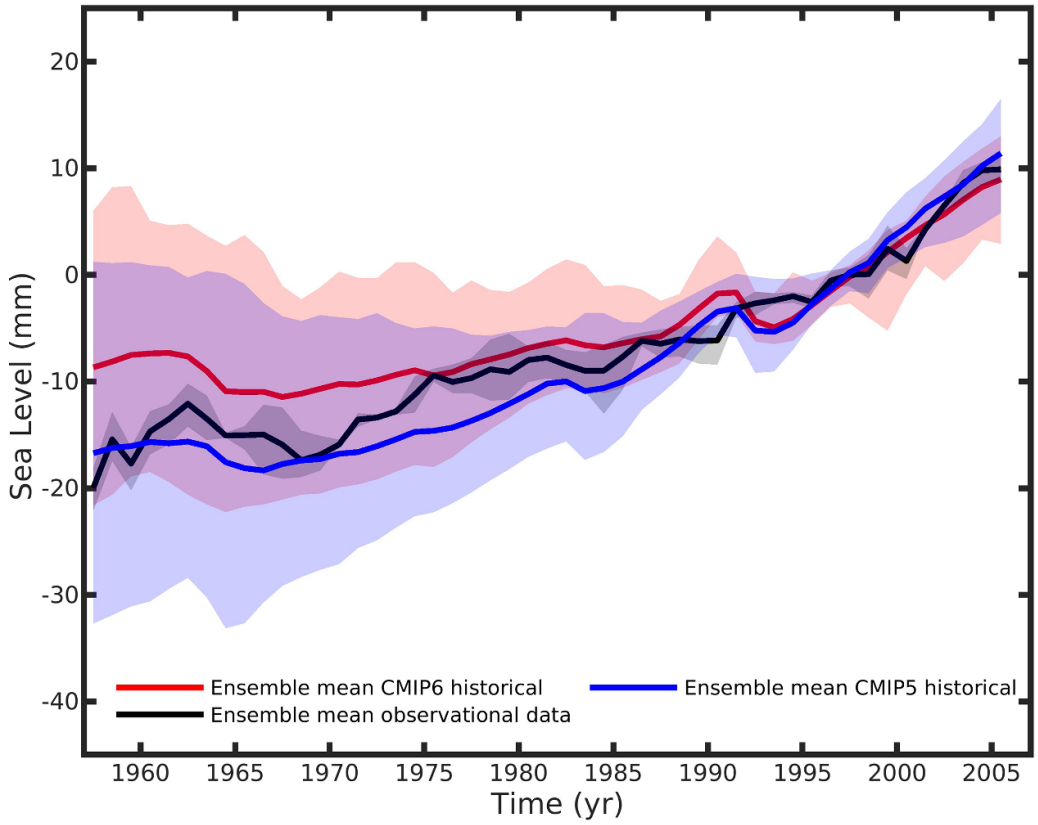

Figure 4. Comparison of CMIP6 and CMIP5 MEMs with ensemble mean observational GMTSL over 1957–2005. The time series have been referenced over 1986–2005. Deep ocean contribution of 0.1 ± 0.1 mm yr^{-1} (available over the period 1990–2000 only), estimated by Purkey and Johnson (2010), is not included in observational GMTSL.

~10 cm per century between historical (since 1901, modelled: purple, observed: black symbols) and projected thermosteric sensitivities for the same rate of change of temperature (e.g. for RCP2.6). Despite this offset, CMIP6 and CMIP5 historical sensitivities show significant overlap though CMIP5 MEM GMTSL sensitivity is higher. When compared to the GMTSL sensitivities simulated by CMIP models with estimates from other sources, the observationally driven thermosteric sea level sensitivities are larger by a few cm per century. The initial response of climate models (Meehl A in figure 5) to SRES A1B aligns well with those in CMIP6 and CMIP5. As the forcing is held constant after 2100 (Meehl *et al* 2007), the climate model's temperature equilibrates quickly resulting in a very small rate of change while the inertia of the ocean heat uptake results in a thermosteric sensitivity with the same magnitude as that of the CMIP5 and CMIP6 future scenarios (Meehl B in figure 5).

4. Discussion

Under the SSP245 and SSP585 scenarios, the CMIP6 models display larger spread in future thermosteric sea level rise by 2100 compared to CMIP5. As discussed in O'Neill *et al* (2016), we expect CMIP6 climate projections to be different from those for CMIP5 due to a new generation of climate models (Eyring *et al* 2016), as well as a new set of scenarios of concentrations, emissions, and land use. One possible explanation for the larger spread in CMIP6 could be that the range of the projected global surface warming is wider in the SSP245 and SSP585 compared to the similar scenario used in CMIP5 (Zelinka *et al* 2020), as changes in GMTSL are related to global surface warming (figure 5). Global surface temperature projections from the selected 15 CMIP6 models, used in this study, show higher temperature changes by 2100 compared to the CMIP5 simulations (figure SI5), supporting the results for 27 CMIP6 in Zelinka *et al* (2020). In addition, for the models used in this study, the CMIP6 mean equilibrium climate sensitivity (ECS) is 3.8 ± 1.2 K, while it is 3.3 ± 0.6 K in CMIP5 (tables SI1 and SI2, based on Meehl *et al* 2020). The transient climate response (TCR) for the models used in the study shows a mean of 2.1 ± 0.5 K in CMIP6 while it is 1.8 ± 0.3 K for CMIP5 (tables SI1 and SI2, based on Meehl *et al* 2020). Thus, the MEM of CMIP6 TCR and ECS are both larger and with a larger spread than for CMIP5.

The response of GMTSL to radiative forcing differs from that of global surface temperature (e.g. Bouttes *et al* 2013). GMTSL depends upon the emissions pathway, in fact Bouttes *et al* (2013) and Melet and Meyssignac (2015) showed that while forcing is positive, GMTSL rise is linearly dependent upon the

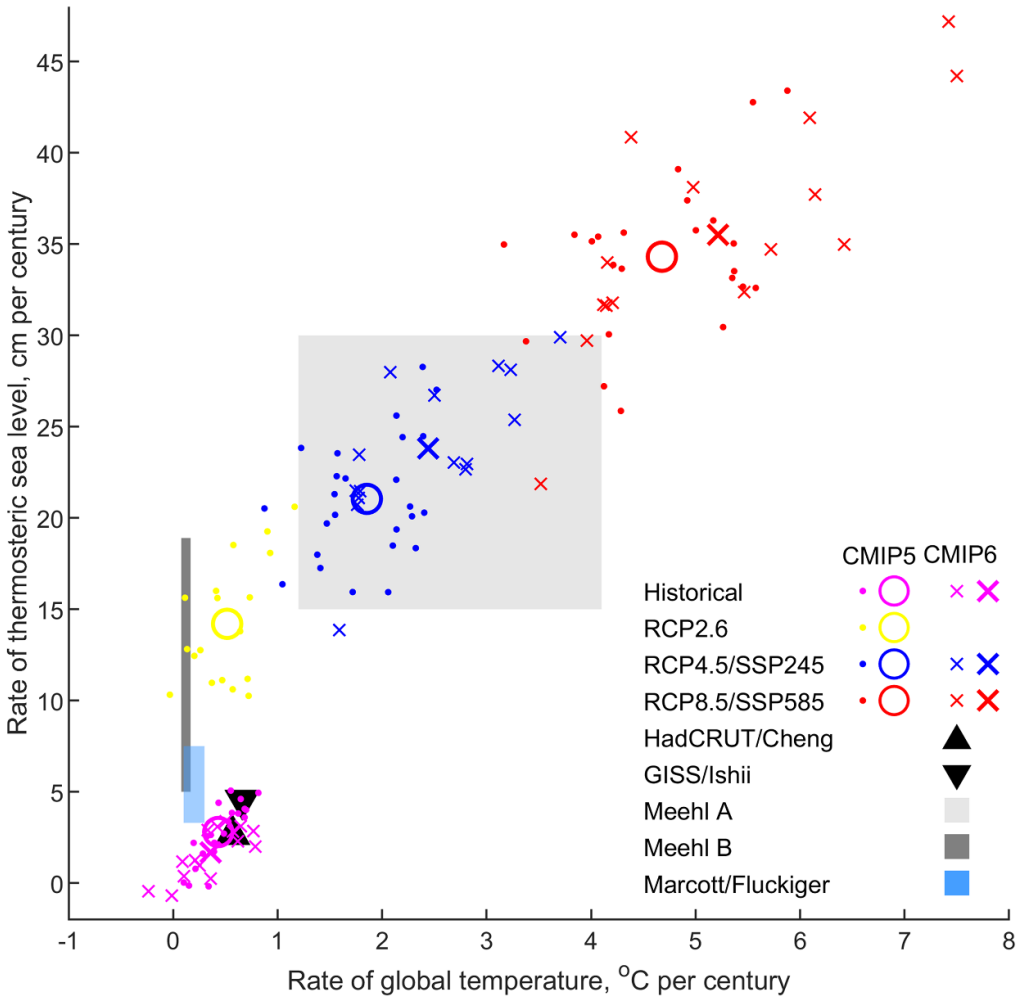

Figure 5. Global mean thermosteric sea level sensitivities (as rate in cm per century) to changes in global surface temperature (°C per century) from model and observational data. Individual models/MEM results for CMIP6 (x/X) and CMIP5 (•/O) for past (1901–1990, magenta) and future (2015–2100) scenarios RCP2.6 (yellow), SSP245/RCP4.5 (blue) and SSP585/RCP8.5 (red). Observational sensitivities (black triangles) using temperature/thermosteric sea level reconstructions (HadCRUT4/Cheng *et al* 2017 and GISTEMP/Ishii and Kimoto 2009). Initial (2000–2100, Meehl A, light grey) and long run (2100–3000, Meehl B, dark grey) sensitivity of climate model simulations under SRES A1B from Meehl *et al* (2007). Sensitivities estimated during early deglacial conditions (light blue) from global temperature reconstruction (Marcott *et al* 2011) and North Atlantic hosing experiments (Fluckiger *et al* 2006).

integral of the forcing. Global surface temperature on the other hand depends roughly linearly upon the forcing (Gregory and Forster 2008). These relations led us to consider the effect of global surface temperature change upon GMTSL over multi-decadal time scales, and whether such analysis helps us to understand both the underestimation of historic GMTSL by both CMIPs and the greater variance of CMIP6 compared to CMIP5.

While this study has primarily considered the sensitivity of GMTSL to global surface warming, ocean heat uptake (and thereby thermosteric sea level) is also influenced by regional changes in ocean dynamics such as the North Atlantic Deep Water formation (Knutti and Stocker 2000) and weakening of AMOC circulation (Cheng *et al* 2019), ocean mixing (Watanabe *et al* 2020) and subduction processes (Griffies and Greatbatch 2012) though such an investigation into their influence is beyond the scope of this paper. While heat redistribution and transport in the ocean play an important part in its warming (Winton *et al* 2013, Zanna *et al* 2019, Cheng *et al* 2019), other reasons for greater sensitivity and ensemble spread include model resolution, numerical schemes and parameterizations (Kirtman *et al* 2012, Eyring *et al* 2016). Using the directly calculated zostoga parameter from CMIP6 may introduce a bias for the historical period in some models due to inclusion/exclusion of marginal seas in calculation of the GMTSL, as it has been suggested in the studies using selected CMIP5 models (e.g. CMIP5 models GFDL-CM3, MIROC-ESM, and GISS-E2-R in Slangen *et al* 2017; not used in this study). The difference up to 0.1 mm yr^{-1} in GMTSL trends for some individual model simulations could be explained by omitting volcanic forcing in pre-industrial runs, but including it in historical simulations. This might lead to differences during historical simulations and projections,

as discussed in Melet and Meyssignac (2015) and Slangen *et al* (2017).

Estimated MEM rates of GMTSL in CMIP6 are smaller than those for CMIP5 from 1901 to 1990 and the difference in rates is statistically significant, which contrasts with the CMIP6 rate for the projections (2015–2100) being higher than in CMIP5. If we check individual models, it is hard to explain why some models do not show any GMTSL rise over the 20th century (e.g. NorESM2, figure SI6 and table SI1) while their future projections are very close to the ensemble mean. If we consider the link between the model simulations of GMTSL to the ECS (not shown here), it is only for the high emission scenario (SSP585) that we can demonstrate an obvious connection between the highest estimate for projected GMTSL and a high ECS in the models. However, for the historical period (1901–1990) there is no noticeable relationship between the GMTSL simulations by CMIP6 models and ECS. This could be explained by the differences in the CMIP6 model response to the radiative forcing for the historic period (e.g. 1850–2000) and forcing for the future projections by 2100, supported by the differences in relative uncertainties for historic and for future periods (figure 3).

Forcing in future scenarios (e.g. SSP245 and SSP585) is dominated by the increase in CO_2 and other greenhouse gas concentrations (O'Neill *et al* 2016). For the 'historical' simulations, in addition to the anthropogenic CO_2, natural forcing occurs as well including the variability of solar irradiance, 'volcanic' aerosol injected into the stratosphere by explosive volcanic eruptions, and anthropogenic aerosols (O'Neill *et al* 2016; Meehl *et al* 2007).

The climate response to volcanic forcing differs between atmosphere and ocean. For a few years following an eruption, volcanic aerosols cause a net negative radiative forcing of the climate system by reflecting sunlight (shortwave radiation) though this is partly offset by absorption of outgoing longwave radiation by the volcanic aerosol (Forster and Taylor 2006). In the ocean, the response to a single (Pinatubo-like) eruption comprises two primary time scales: one fast (1–2 years) and one slow (decadal). Over the fast time scale, the ocean sequesters cooling anomalies induced by the eruption into its depth, enhancing the damping rate of sea surface temperature relative to that which would be expected if the atmosphere acted alone (Gupta and Marshall 2018). However, because of its large effective heat capacity, the ocean memory of successive eruptions enables an accumulation larger than any single event (e.g. Hansen *et al* 2002, Grinsted *et al* 2007, Stenchikov *et al* 2009). This complex response by the ocean to the forcing during the historical period could provide some explanation for relatively lower sensitivity of GMTSL rise to the changes in global surface temperature (figure 5).

Further studies that focus on developing an understanding of large uncertainties in heat uptake by the ocean in climate models (AOGCMs and ESMs) within CMIP6 would greatly contribute to the improvement of future sea level projections given the important role played by oceans in the storage and redistribution of heat and to modulate future changes in climate (Melet and Meyssignac 2015, Gregory *et al* 2020, Todd *et al* 2020).

5. Conclusion

We estimate a GMTSL rise of 18.8 cm (12.8–23.6 cm, 5–95th percentile) and up to 26.8 cm (18.6–34.6 cm, 5–95th percentile) by the end of the 21st century with SSP245 and SSP585 scenarios, respectively. Our study provides evidence that despite huge improvements in current AOGCMs and ESMs (O'Neill *et al* 2016, Eyring *et al* 2016) CMIP6 models show larger disagreement in projecting the GMTSL by 2100 compared to CMIP5 simulations, which will by extension create larger uncertainties in total, global and regional sea level projections. Over the historical time (since 1900) the comparisons with observed and reconstructed GMTSL show that overall CMIP6 models and CMIP6 MEM are underestimating the observed GMTSL.

Given the importance of GMTSL to sea level projections, an improved understanding of the causes of model spread and the role of natural variability and external forcing therein needs to be a high priority in the climate and sea level rise modelling community. As more outputs from CMIP6 models become available, more detailed analysis of GMTSL will be possible. On the other hand, evaluating model performance (by comparison with instrumental records) will remain limited by the lack of long-term historical observations of temperature and salinity in the ocean.

Data availability statement

The data that support the findings of this study are available upon reasonable request from the authors.

Acknowledgments

We acknowledge the World Climate Research Programme's Working Group on Coupled Modelling for providing the CMIP6 and CMIP5 archive and the climate modelling groups for providing their outputs. L P J acknowledges funding from the Robertson Foundation for Climate Econometrics (Grant Nos.: 9907422 and 9908921).

ORCID iD

Svetlana Jevrejeva https://orcid.org/0000-0001-9490-4665

References

Abadie L M, Jackson L P, Sainz de Murieta E, Jevrejeva S and Galarraga I 2020 Comparing urban coastal flood risk in 136 cities under two alternative sea-level projections: RCP 8.5 and an expert opinion-based high-end scenario *Ocean Coast. Manag.* **193** 105249

Bouttes N, Gregory J M and Lowe J A 2013 The reversibility of sea level rise *J. Clim.* **26** 2502–13

Cheng L, Abraham J, Hausfather Z and Trenberth K E 2019 How fast are the oceans warming? *Science* **363** 128–9

Cheng L, Trenberth K E, Fasullo J, Boyer T, Abraham J and Zhu J 2017 Improved estimates of ocean heat content from 1960 to 2015 *Sci. Adv.* **3** e1601545

Church J A *et al* 2013 Sea level change *Climate Change 2013: The Physical Science Basis. Contribution of Working Group I to the Fifth Assessment Report of the Intergovernmental Panel on Climate Change*, ed T F Stocker, D Qin, G-K Plattner, M Tignor, S K Allen, J Boschung, A Nauels, Y Xia, V Bex and P M Midgley (Cambridge: Cambridge University Press)

Eyring V, Bony S, Meehl G A, Senior C A, Stevens B, Stouffer R J and Taylor K E 2016 Overview of the Coupled Model Intercomparison Project Phase 6 (CMIP6) experimental design and organization *Geosci. Model Dev.* **9** 1937–58

Fluckiger J, Knutti R and White J 2006 Oceanic processes as potential trigger and amplifying mechanisms for Heinrich events *Paleoceanography* **21** PA2014

Forster P M de and Taylor K E 2006 Climate forcings and climate sensitivities diagnosed from coupled climate model integrations *J. Climate* **19** 6181–94

Frederikse T *et al* 2020 The causes of sea-level rise since 1900 *Nature* **584** 393–7

GISTEMP Team 2020 GISS Surface Temperature Analysis (GISTEMP), version 4 NASA Goddard Institute for Space Studies Dataset (available at: https://data.giss.nasa.gov/gistemp/) (Accessed 09 July 2020)

Gregory J M *et al* 2019 Concepts and terminology for sea level-mean, variability and change, both local and global *Surv. Geophys.* **40** 1251–89

Gregory J M, Andrews T, Ceppi P, Mauritsen T and Webb M J 2020 How accurately can the climate sensitivity to CO2 be estimated from historical climate change? *Clim. Dyn.* **54** 129–57

Gregory J M and Forster M 2008 Transient climate response estimated from radiative forcing and observed temperature change *J. Geophys. Res.* **113** D23105

Gregory J M and Lowe J A 2000 Predictions of global and regional sea-level rise using AOGCMs with and without flux adjustment *Geophys. Res. Lett.* **27** 3069–72

Griffies S M *et al* 2016 OMIP contribution to CMIP6: experimental and diagnostic protocol for the physical component of the Ocean Model Intercomparison Project *Geosci. Model Dev.* **9** 3231–96

Griffies S M and Greatbatch R J 2012 Physical processes that impact the evolution of global mean sea level in ocean climate models *Ocean Modelling* **51** 37–72

Grinsted A, Moore J C and Jevrejeva S 2007 Observational evidence for volcanic impact on sea level and the global water cycle *PNAS* **104** 19730–4

Gupta M and Marshall J 2018 The climate response to multiple volcanic eruptions mediated by ocean heat uptake: damping processes and accumulation potential *J. Clim.* **31** 8669–87

Hansen J *et al* 2002 Climate forcings in Goddard Institute for Space Studies SI2000 simulations *J. Geophys. Res.* **107** 4347

Ishii M and Kimoto M 2009 Reevaluation of historical ocean heat content variations with time-varying XBT and MBT depth bias corrections *J. Oceanogr.* **65** 287–99

Jackson L P and Jevrejeva S 2016 A probabilistic approach to 21st century regional sea-level projections using RCP and High-end scenarios *Glob. Planet. Change* **146** 179–89

Jevrejeva S *et al* 2019 Probabilistic sea level projections at the coast by 2100 *Surv. Geophys.* **40** 1673–96

Kirtman B P *et al* 2012 Impact of ocean model resolution on CCSM climate simulations *Clim. Dyn.* **39** 1303–28

Knutti R and Stocker T F 2000 Influence of the thermohaline circulation on projected sea level rise *J. Clim.* **13** 1997–2001

Kopp R E, Horton R M, Little C M, Mitrovica J X, Oppenheimer M, Rasmussen D J, Strauss B H and Tebaldi C 2014 Probabilistic 21st and 22nd century sea-level projections at a global network of tide-gauge sites *Earth's Future* **2** 383–406

Lenssen N J L *et al* 2019 Improvements in the GISTEMP uncertainty model *J. Geophys. Res. Atmos.* **124** 6307–26

Levitus S *et al* 2012 World ocean heat content and thermosteric sea level change (0–2000 m), 1955–2010: world ocean heat content *Geophys. Res. Lett.* **39** n/a-n/a

Marcott S A *et al* 2011 Ice-shelf collapse from subsurface warming as a trigger for Heinrich events *Proc. Natl Acad. Sci. USA* **108** 13415–9

Meehl G A *et al* 2020 Context for interpreting equilibrium climate sensitivity and transient climate response from the CMIP6 Earth system models *Science* **6** eaba1981

Meehl G A *et al* 2007 Global climate projections *Climate Change 2007: The Physical Science Basis Contribution of Working Group I to the Fourth Assessment Report of the Intergovernmental Panel on Climate Change*, ed S Solomon, D Qin, M Manning, Z Chen, M Marquis, K B Averyt, M Tignor and H L Miller (Cambridge: Cambridge University Press)

Melet A and Meyssignac B 2015 Explaining the spread in global mean thermosteric sea level rise in CMIP5 climate models *J. Clim.* **28** 9918–40

Morice C P, Kennedy J J, Rayner N A and Jones P D 2012 Quantifying uncertainties in global and regional temperature change using an ensemble of observational estimates: the HadCRUT4 data set *J. Geophys. Res.* **117** D08101

Nowicki S M J *et al* 2016 Ice Sheet Model Intercomparison Project (ISMIP6) contribution to CMIP6 *Geosci. Model Dev. Discuss.* **9** 4521–45

O'Neill B P *et al* 2016 The Scenario Model Intercomparison Project (ScenarioMIP) for CMIP6 *Geosci. Model Dev.* **9** 3461–82

Oppenheimer M *et al* 2019 Sea level rise and implications for low-lying islands, coasts and communities *IPCC Special Report on the Ocean and Cryosphere in a Changing Climate*, ed H-O Pörtner, D C Roberts, V Masson-Delmotte, P Zhai, M Tignor, E Poloczanska, K Mintenbeck, A Alegría, M Nicolai, A Okem, J Petzold, B Rama and N M Weyer

Purkey S G and Johnson G C 2010 Warming of global Abyssal and deep southern ocean waters between the 1990s and 2000s: contributions to global heat and sea level rise budgets *J. Clim.* **23** 6336–51

Sen Gupta A, Jourdain N C, Brown J N and Monselesan D 2013 Climate drift in the CMIP5 Models* *J. Clim.* **26** 8597–615

Slangen A B A *et al* 2017 Evaluating model simulations of 20th century sea-level rise. Part 1: global mean sea-level change *J. Clim.* **30** 8539–63

Stenchikov G, Delworth T L, Ramaswamy V, Stouffer R J, Wittenberg A and Zeng F 2009 Volcanic signals in oceans *J. Geophys. Res.* **114** D16104

Storto A *et al* 2019 Ocean reanalyses: recent advances and unsolved challenges *Front. Mar. Sci.* **6** 418

Taylor K E *et al* 2012 An overview of CMIP5 and the experiment design *Bull. Am. Meteorol. Soc.* **93** 485–98

Todd A *et al* 2020 Ocean-only FAFMIP: understanding regional patterns of ocean heat content and dynamic sea level change *J. Adv. Modell. Earth Syst.* **12** e2019MS002027

Vousdoukas M I et al 2018 Global probabilistic projections of extreme sea levels show intensification of coastal flood hazard *Nat. Commun.* **9** 2369

Watanabe M et al 2020 Control of transient climate response and associated sea level rise by deep-ocean mixing *Environ. Res. Lett.* **15** 094001

WCRP Global Sea Level Budget Group 2018 Global sea-level budget 1993–present *Earth Syst. Sci. Data* **10** 1551–90

Winton M, Griffies S M, Samuels B L, Sarmiento J L and Frölicher T L 2013 Connecting changing ocean circulation with changing climate *J. Clim.* **26** 2268–78

Yin J 2012 Century to multi-century sea level rise projections from CMIP5 models *Geophys. Res. Lett.* **39** L17709

Zanna L, Khatiwala S, Gregory J M, Ison J and Heimbach P 2019 Global reconstruction of historical ocean heat storage and transport *Proc. Natl Acad. Sci. USA* **116** 1126–31

Zelinka M D, Myers T A, Mccoy D T, Po-Chedley S, Caldwell P M, Ceppi P, Klein S A and Taylor K E 2020 Causes of higher climate sensitivity in CMIP6 models *Geophys. Res. Lett.* **47** e2019GL085782